SETAC PRESS

Environmental Toxicology and Chemistry, Vol. 34, No. 10, pp. 2263–2270, 2015

Printed in the USA

UPTAKE ROUTES AND TOXICOKINETICS OF SILVER NANOPARTICLES AND SILVER IONS IN THE EARTHWORM *LUMBRICUS RUBELLUS*

Maria Diez-Ortiz,*† Elma Lahive,† Peter Kille,‡ Kate Powell,‡ A. John Morgan,‡ Kerstin Jurkschat,§ Cornelis A.M. Van Gestel,|| J. Fred W. Mosselmans,# Claus Svendsen,† and David J. Spurgeon†

†Centre for Ecology and Hydrology, Crowmarsh Gifford, Wallingford, Oxfordshire, United Kingdom
‡Cardiff School of Biosciences, University of Cardiff, Cardiff, Wales, United Kingdom
§Department of Materials, Oxford University, Yarnton, Oxfordshire, United Kingdom
||Department of Ecological Science, Faculty of Earth and Life Sciences, VU University, Amsterdam, The Netherlands
#Diamond Light Source, Harwell Science and Innovation Campus, Didcot, Oxfordshire, United Kingdom

(Submitted 16 June 2014; Returned for Revision 14 August 2014; Accepted 24 April 2015)

Abstract: Current bioavailability models, such as the free ion activity model and biotic ligand model, explicitly consider that metal exposure will be mainly to the dissolved metal in ionic form. With the rise of nanotechnology products and the increasing release of metal-based nanoparticles (NPs) to the environment, such models may increasingly be applied to support risk assessment. It is not immediately clear, however, whether the assumption of metal ion exposure will be relevant for NPs. Using an established approach of oral gluing, a toxicokinetics study was conducted to investigate the routes of silver nanoparticles (AgNPs) and Ag^+ ion uptake in the soil-dwelling earthworm *Lumbricus rubellus*. The results indicated that a significant part of the Ag uptake in the earthworms is through oral/gut uptake for both Ag^+ ions and NPs. Thus, sealing the mouth reduced Ag uptake by between 40% and 75%. An X-ray analysis of the internal distribution of Ag in transverse sections confirmed the presence of increased Ag concentrations in exposed earthworm tissues. For the AgNPs but not the Ag^+ ions, high concentrations were associated with the gut wall, liver-like chloragogenous tissue, and nephridia, which suggest a pathway for AgNP uptake, detoxification, and excretion via these organs. Overall, the results indicate that Ag in the ionic and NP forms is assimilated and internally distributed in earthworms and that this uptake occurs predominantly via the gut epithelium and less so via the body wall. The importance of oral exposure questions the application of current metal bioavailability models, which implicitly consider that the dominant route of exposure is via the soil solution, for bioavailability assessment and modeling of metal-based NPs. *Environ Toxicol Chem* 2015;34:2263–2270. © 2015 SETAC

Keywords: Silver Nanoparticles Exposure route Uptake X-ray absorption near-edge spectroscopy

INTRODUCTION

Because of the rapid increase in nanotechnology, engineered nanoparticles (NPs) can be expected to enter the environment at increased rates. The nature of some common nanotechnology products (including cosmetics, textiles, and personal care products) means that NPs will enter wastewater streams, where within sewage systems they may sediment into the sludge material. The deposition of this waste to land provides a route by which these released NPs may enter soil ecosystems [1–3]. Once in the environment, there is the potential for metal-based NPs or metal ions, which are derived following their solubilization, to come into contact with organisms and hence to be accumulated [4–7].

The prevailing ecotoxicology paradigm states that for effects to occur it is necessary for the material to be taken up into the body, and ultimately reach a target site. For conventional chemicals, the concepts of toxicokinetics and toxicodynamics are well established as a coherent framework that links exposure to toxic effects [8]. There is reason to expect that this paradigm will be relevant for NPs, although some debate remains concerning the extent to which toxicity may be dependent on the biological interactions that will result once NPs enter tissues and cells. Hence, to understand the effects of NPs, it is important to understand key aspects governing uptake into exposed organisms under realistic conditions.

For organisms that live in soils, NP exposure can be expected to occur through 3 main routes. Exposure through air is relevant only for more volatile chemicals and hence for NPs under normal soil moisture conditions, it is unlikely to be important. For the remaining 2 routes, namely, exposure through contact with and transfer across the skin (dermal) and ingestion and transfer across the gut epithelium (oral), previous studies with conventional chemicals have generally suggested that dermal exposure is the dominant route. This includes pesticides and nonpolar organic chemicals in studies with woodlice and earthworms [9] and for Cd and Zn metal ions in a classic study by Vijver et al. [10] that used surgical glue to inhibit soil ingestion. The latter approach allowed for separate analysis of dermal uptake with and without the additional inputs derived from ingestion and is adopted in the present study.

Indications of dermal contact as the dominant route of exposure have underpinned the development of models such as the free ion activity model [11] and later the biotic ligand model (BLM) [12] and related terrestrial bioavailability methods that link soil solution chemistry and metal speciation modeling to passive absorption and surface ligand binding on biological membranes, notably the epidermis and gill and thereafter ultimately to toxic effects [11–14]. The successful application of these models to explain the effects of variations in media properties on metal toxicity [15–17] has pointed to the validity of their inherent assumptions, with exposure mainly through external body surfaces. However, although many studies have

* Address correspondence to mdiez@leitat.org
Published online 27 April 2015 in Wiley Online Library (wileyonlinelibrary.com).
DOI: 10.1002/etc.3036

used the free ion activity model and BLM to explain metal bioavailability and toxicity, not all research has necessarily supported this conjecture regarding exposure routes. For example, the results of Cain et al. [18] suggested that free ion concentrations accounted for less than 5% of Cd and Cu accumulation in mayflies in aqueous exposure. In addition, identification of a dependence of uptake on gut physiology and microbiome composition [19,20] indicates that dietary uptake is an important exposure route [21].

Previous studies of soil invertebrate exposure to metal-based NPs have established that these materials can enter tissues either as intact particles or following dissociation to ions [6,22,23]. In cases where the uptake of intact NPs is suggested, it is, however, currently unclear how these materials enter tissues. This uncertainty currently places limits on the development of a modeling framework that can link NP exposure to uptake and effects, such as, for example whether assumptions of dermal uptake are valid. To specifically assess the importance of different potential exposure routes of NP uptake, we conducted the present study to assess the toxicokinetic patterns of Ag uptake in earthworms exposed to both ionic and NP forms of Ag in soil, using the same oral sealing approaches as used by Vijver et al. [10] to quantify the comparative contributions of both the dermal and oral exposure route.

MATERIALS AND METHODS

Material supply and characterization

Uptake studies were conducted with 2 chemical forms of Ag, silver nanoparticles (AgNPs), and Ag^+ ions derived from $AgNO_3$. The AgNPs were obtained from NanoTrade. The material had an indicated average particle size of 50 nm and had no coatings or surface modifications. It was supplied as a white odorless dry powder. For initial material characterization, dispersions of the material (1 mg mL^{-1}) were prepared in distilled water for particle morphology and size distribution analyses using transmission electron microscopy (TEM). For the analysis, a drop of the water dispersion was deposited on a holey carbon-coated Cu TEM grid and dried at room temperature for several hours before examination. The instrument used was a JEOL 2010 analytical TEM incorporating an LaB6 electron gun operating between 80 kV and 200 kV and equipped with an Oxford Instruments LZ5 windowless energy dispersive X-ray spectrometer. The Ag nitrate salt ($AgNO_3$, 99% purity) used was purchased from BHD Chemicals as a white crystalline powder.

Soil selection and spiking

The soil used for all Ag uptake kinetic studies was standardized LUFA 2.2 loam sand (LUFA-Speyer) [24]. Analysis of the single purchased batch used for all experiments indicated that this soil had a pH of 5.5 ± 1.1 in a 3:1 water:soil slurry, an organic carbon content of 2.1 ± 0.4 w/w %, a cation exchange capacity of 10 ± 0.5 mEq 100 g^{-1}, and a water holding capacity of 55%. The soil was initially screened through a 2-mm mesh to remove any large coarse material and to break up larger aggregates. The batch was then subdivided into sufficient aliquots for each control, AgNP-spiked, and Ag^+ ion treatment replicate.

The test soils were spiked with the uncoated AgNPs and Ag^+ ions (as $AgNO_3$) at 2 different nominal concentrations for each of the 2 silver forms (20 mg Ag kg^{-1} and 100 mg Ag kg^{-1} for $AgNO_3$ and 100 mg Ag kg^{-1} and 500 mg kg^{-1} for AgNPs). Previous work conducted to assess the toxicity of freshly spiked pristine AgNPs and freshly spiked Ag^+ ions have generally shown a greater toxicity of the ionic Ag [25]. For this reason, the toxicokinetics studies were conducted using different exposure concentrations for the 2 Ag forms. For the putatively less toxic AgNPs, a higher exposure concentration of 500 mg Ag kg^{-1} and lower value of 100 mg Ag kg^{-1} were chosen. For the Ag^+ ions, the highest concentration used was 100 mg Ag kg^{-1} and the lower value was 20 mg Ag kg^{-1}. The higher concentrations used were selected to provide a relatively high exposure level to ensure detection of uptake. The second concentration was then selected at 20% of this higher value to allow investigation of uptake at levels below those likely to cause overt toxicity. Use of a common value of 100 mg Ag kg^{-1} dry weight for both forms allowed direct comparison between the 2 Ag forms. Additional replicates of the unspiked test soils were prepared (control samples). Samples collected from the control treatment were used to confirm that all accumulated metal in the spiked soils related to the Ag added and not to assimilation of residual material in the soil.

The same dosing technique was used to spike both silver forms into the test soil. Because there were problems with maintaining a stable dispersion of the AgNPs in distilled water, direct dry dosing of the powder into the soil was selected as the most suitable option to obtain a homogenous Ag distribution [26]. This method was also used to spike the soils with the $AgNO_3$. The AgNPs and solid crystalline $AgNO_3$ were initially mixed into a dried subsample of the test soil. These dosed aliquots were then thoroughly mixed with the remaining soil to give the 200 g of spiked soil used for each test replicate. Spiked soils were then wetted with Milli-Q water to a soil moisture content of 45% of maximum water holding capacity [27]. After a further mixing, all soils were maintained for an initial period of 1 wk to allow for the initial binding and interactions of the added AgNPs and ions with soil solid phase and porewater components.

To validate background and added nominal Ag concentrations, samples were taken from a selection of the test replicates over the experimental period. These soil samples ($\sim$20 g) were initially oven dried at 80 °C, and then a 100-mg aliquot of this sample was digested in 2 mL of a 4:1 mixture of hydrochloric acid (37% p.a., Baker, Grainger) and nitric acid (65% p.a., Riedel-de-Haen) in closed Teflon bombs heated at 140 °C for 7 h. Digests were diluted with 8 mL of deionized water and analyzed for total Ag by flame atomic absorption spectroscopy (PerkinElmer AAnalyst 100). For quality assurance purposes, a certified reference material (River Clay, WEPAL-ISE-886) and reagent blanks were also analyzed. The averages of measured Ag concentrations were within 25% of the certified reference value (River Clay contains 2.8 ± 0.4 mg Ag kg^{-1}; silver concentrations in the certified reference material ranged between 2.6 mg Ag kg^{-1} and 3.9 mg Ag kg^{-1} dry wt). No Ag was detected in the blank samples. The experimental detection limit for the Ag measurements was 0.3 mg kg^{-1}.

Soil porewater samples were also collected for Ag analysis from separately prepared replicate soil samples by centrifugation (J2-HC, Beckman Coulter) for all 4 Ag treatments assessed. A 50-g batch of spiked soils was taken from these 4 replicates and saturated with 13.5 mL of Milli-Q water and centrifuged for 60 min at 4000 *g* [7]. The samples (supernatants) were then acidified and analyzed for total Ag concentration by flame atomic absorption spectroscopy (PerkinElmer AAnalyst 100).

Uptake bioassay and tissue Ag analysis

All earthworms used were morphologically determined to be *Lumbricus rubellus* (supplied by Lasebo). This species was

chosen because it is a widely distributed epigeic earthworm species in agricultural soils, where it may come into contact with Ag in NP and ionic forms added through routes such as sewage sludge. Furthermore, *L. rubellus* has also been found to be suitable for oral gluing studies [10]. All earthworms were initially maintained in a stock culture on a medium consisting of 1:1:1 mix of composted bark: *Spagnum* peat:loam soil and supplied ad libitum with a combination of horse manure collected from animals that grazed on uncontaminated pasture and that had not undergone any recent medication and additional vegetable peelings supplied as food. Selected earthworms used for the experiment were taken from this stock culture. All earthworms were adults with well-developed clitella.

Of the earthworms selected for the present study's experiment, half were subjected to oral sealing to prevent soil ingestion and, hence, exposure through the digestive tract. Sealing was achieved by covering the mouth parts in the first segment of the earthworm with medical histoacryl glue (Braun Aesculap). The glue was applied by dipping the earthworm's mouth in the glue as described in detail in the original study [10]. Following gluing, all sealed and unsealed individuals were placed individually onto the surface of the unspiked and AgNP- and Ag^+ ion-spiked soil. A total of 44 sealed and 44 unsealed earthworms were used for each of these treatments (2 × NP; 2 × ionic; 1 × reference) to provide a sufficient number of individuals for collection of 4 replicate earthworms for each of the 10 exposure times used for the uptake study. Four worms with individual fresh weights ranging from 1.15 g to 2.02 g (average ± SD, 1.62 ± 0.21 g) were placed into glass jars containing approximately 360 g of dry soil. All containers were checked after 1 h to ensure that the earthworms had burrowed into the test soil. Containers were then incubated at 12 ± 1 °C in a 16:8-h light:dark regime for a total of 168 h to allow accumulation of the different Ag forms. Earthworms were not fed during the experiment. Soil moisture loss was checked and if necessary corrected over the exposure period. Exposures were stopped after 168 h to be sure that we were avoiding the time point from which earthworms could start experiencing physiological changes linked to starvation.

At 0 h (i.e., worms taken from batch at the start of exposure), 4 h, 8 h, 24 h, 36 h, 48 h, 72 h, 96 h, 120 h, and 168 h after initiation, 4 sealed and 4 unsealed individuals were removed from containers for each of the 5 treatments. Collected earthworms were rinsed, blotted dry on filter paper, and weighed. The earthworms were then kept individually for 36 h in Petri dishes lined with a piece of moistened filter paper to allow them to void their gut content. To restrict coprophagy, the filter paper was changed after 24 h. The amount of excreta produced on filter paper by the sealed earthworms was checked. Only in 4 cases did sealed worms excrete soil particles; these worms were excluded from further analyses. The earthworms were then snap-frozen and freeze-dried for 2 d, and the dried tissue was weighed. The whole tissue was then digested in 2 mL of a 1:4 mixture of nitric acid (65% p.a.; Riedel-de-Haen) and hydrochloric acid (37% p.a., Baker) in tightly closed Teflon bombs on heating in a destruction oven at 140 °C for 7 h, and the Ag concentration was measured by flame atomic absorption spectrometry (PerkinElmer Analyst 100). A biological reference material Dogfish Liver, DOLT-4, having a certified concentration of 0.93 ± 0.07 mg Ag kg^{-1} dry weight was included as a quality check. Measured concentrations of this material were between 80% and 120%, with average recovery 97%.

μX-ray fluorescence mapping

Bioimaging was performed at the Diamond Light Source (Didcot, UK) using the I18 beamline. Fresh tissue samples taken from the midintestinal region of earthworms exposed for 168 h to AgNPs (500 mg Ag kg^{-1}) and Ag^+ ions (100 mg Ag kg^{-1}) were processed by overnight fixation in 70% ethanol, embedded in glycol methacrylate resin, and sectioned at 8 μm with a tungsten-coated steel knife. Sections were mounted on Ultralene® 4-μm-thick window film (SPEX SamplePrep) stretched across a hole in a plastic slide to minimize the Si signal associated with glass substrates. Slides were inserted into the standard I18 sample holder, and imaged externally under brightfield conditions for orientation purposes.

X-ray fluorescence data were collected using a Si(111) double crystal monochromator, and the Kirkpatrick–Baez focusing mirrors, which provided a 3-μm spot size, were also used to remove harmonic contamination. The sample holder was positioned at 45 °C to the incident beam. The Ag K-edge at 25.531 eV is above the dynamic range of the I18 beamline, and the Ag L(III)-edge Lα line is very close to the argon Kα line; hence the Ag L(II)-edge at 3.540 eV was used. This provides a relatively insensitive signal, however, as the Ag L(III)-edge has a low fluorescence yield [28]. Data were recorded using a 4-element Si drifts detector (Hitachi) positioned close to the specimen, whereas the Ar signal (from ambient air) was reduced but not eliminated by enclosing the specimen and detector inside a bespoke bag under flowing He to give a largely He environment during analysis. Two X-ray fluorescence maps over the same region of the sample were collected using an incident energy below the Ag L(II)-edge at 3500 eV and one above the edge at 3580 eV. The signal in the Ag Lβ energy window in the lower energy map was subtracted from the signal in the higher energy map in PyMca 4.1.1 [29], to remove the signal observed from the argon Kβ line and produce the Ag X-ray fluorescence map. The Ag X-ray fluorescence maps were acquired but spot X-ray absorption near-edge spectroscopy (μXANES) scans at the Ag L(II)-edge XANES spectra are not of sufficient quality to permit spectral analysis because of the relatively low levels of signal detection from samples.

Data handling and statistical analysis

Uptake and elimination rate constants were estimated by applying a 1-compartment first-order kinetics model to the data for the uptake phase, with a constant start value of C_0. This model has been widely used in the ecotoxicological literature as a means to assess uptake and elimination kinetics. The 1-compartment model fitted to the data took the form:

$$C_w = C_0 + (k_1/k_2) \times C_{exp} \times (1\text{-}e^{-k2\times t}) \quad (1)$$

where t = exposure time (h), C_w = internal concentration in the earthworms (μg g^{-1} dry wt), k_1 = uptake rate constant (g soil g earthworm $^{-1}$ h^{-1}), k_2 = elimination rate constant (h^{-1}), C_0 = initial concentration in the earthworm (mg kg^{-1} dry wt), and C_{exp} = exposure concentration (mg kg^{-1} dry soil). Two sets of values were calculated for the uptake rate; $k_{1\text{-}T}$ was calculated using total measured Ag concentration and $k_{1\text{-}pw}$ using silver concentration in the soil porewater. Equations were fitted to the replicate experimental data using least squared regression fitting in SPSS 17.1. From model fits, all parameter values including standard errors and/or confidence intervals and coefficient of determination (r^2) values indicating goodness of fit were derived. Significant differences between uptake rates for sealed and

unsealed earthworms were compared using a generalized likelihood ratio test [30].

RESULTS

Material characterization and concentration validation

The TEM analysis of the supplied nanopowder indicated the presence of primary particles in the 50-nm to 80-nm range, with a smaller proportion of smaller 10-nm to 30-nm particles. These primary particles had often formed into loose agglomerates. These were not, however, stable structures as they were readily disintegrated by exposure to the TEM electron beam during analysis. Furthermore, characterization of these materials can be found in Diez et al. [31].

Silver concentrations in control soil were below the method detection limit of 0.3 mg kg^{-1}. The average measured Ag concentrations in replicate soil samples from each treatment were >85% of nominal values, confirming the general efficiency of the spiking procedure (Table 1). The Ag concentrations in porewater samples were 10 times higher for the soil spiked with ionic Ag than in soil spiked with AgNPs at the same total nominal Ag concentrations (100 mg kg^{-1}; Table 1).

Ag uptake in sealed and unsealed earthworms

During the experiments, the burrowing capacity of sealed and unsealed earthworms was similar, and they all disappeared into the soil. No obvious visual differences in activity and locomotion were found, although initially the sealed earthworms needed approximately 15 min to begin burrowing. Hence the extent of dermal contact with the soils was not affected, when oral exposure was prevented. No effect on survival was observed during the 96-h exposure period.

The Ag concentrations in earthworms exposed to the unspiked soil were low (average Ag concentration was 0.02 μg g^{-1} dry wt) over the duration of the exposure. This is consistent with the low background Ag levels found in this soil and confirms that the patterns of uptake seen are not the result of the accumulation of any background metal. The Ag concentrations in *L. rubellus* exposed to both Ag forms increased with time (Figure 1). For all 8 datasets for sealed and unsealed earthworms at 2 concentrations of Ag^+ ions and NPs, Ag uptake patterns could be described by the 1-compartment model. There was, however, significant interindividual variation between earthworms. As a consequence, the proportion of total variation explained by the model was relatively modest ($r^2 = 0.290$–0.815).

For unsealed worms, 1-compartment model fits indicated that uptake rates ($k_{1\text{-T}}$ and $k_{1\text{-pw}}$) were greater at the higher exposure concentrations in earthworms exposed to Ag ions (Table 2), whereas nonsignificant differences were found after exposure to different concentrations of AgNPs ($p < 0.05$). The earthworms that were subject to oral sealing with surgical glue also assimilated Ag from both forms of Ag (Figure 1). The Ag uptake seen for the AgNPs, both with and without the potential for oral exposure, is not in itself indicative of direct NP uptake, because assimilation may be of the ions produced by dissolution. A comparison of parameters for the earthworms exposed to 100 mg kg^{-1} of Ag^+ ions and AgNPs indicated significantly higher uptake rates (k_1) for the ionic treatment ($p < 0.05$, Table 2).

Even though there was assimilation of Ag from soil in sealed earthworms, inhibition of ingestion resulted in a substantial reduction in uptake of both Ag forms. Thus, after 168 h, Ag tissue concentrations in sealed earthworms were between 40% and 75% of those in unsealed individuals across both Ag forms and exposure levels (Figure 1). This finding suggests that for both AgNPs and Ag^+ ions, soil ingestion is a major route of exposure. Thus, in unsealed earthworms, body concentration reached equilibrium after 48 h to 72 h after exposure to Ag^+ ion, but not until after 96 h in AgNP exposures. In sealed earthworms, tissue Ag levels increased throughout the exposure period and did not reach equilibrium within 96 h for both Ag forms (Figure 1).

Elimination rate constants in all cases were low and close to 0, and they were similar in both sealed and unsealed worms exposed to silver ions and silver nanoparticles at 100 mg kg^{-1}, suggesting that the elimination route might be similar independently of the exposure route.

The Ag uptake by both unsealed and sealed earthworms raises questions regarding the target organs for Ag sequestration, and whether Ag was more efficiently accumulated within specific tissues following experimental exposure for intact AgNPs or for Ag^+ ions. To help address these questions, tissues of unsealed earthworms were analyzed using synchrotron μX-ray fluorescence. The tissue-specific in situ distribution of Ag, sulfur (S), and phosphorus (P) was derived for unsealed worms exposed to 500 mg kg^{-1} AgNPs (Figure 2A and 2C) and unsealed worms exposed to 100 mg Ag kg^{-1} of Ag+ ions (Figure 2B and 2D). Alcohol-fixed, methacrylate-embedded transverse sections (10 μM) were imaged directly using a light microscope, and an area was identified for μX-ray fluorescence mapping that included the majority of earthworm organs involved in metal sequestration and excretion (Figure 2A and 2B; areas shown by the perimeter of the black rectangle). Elemental distributions were derived using μX-ray fluorescence mapping performed under a helium environment, to minimize the interference of argon K-edge. Elemental fluorescence spectra were modeled, and any residual contribution of Ar was removed by spectral subtraction. This enabled us to overlay the distribution of Ag (shown in blue) with S (green) and separately P (red), which provided us with the anatomical location of the Ag. To confirm the presence of Ag, we acquired XANES scans across the Ag L(II)-edge at specific points within tissues derived from AgNPs and Ag ions (Figure 2C and 2D). These showed that in NP-exposed unsealed earthworms Ag (Lβ) fluorescence was

Table 1. Nominal, measured, and porewater concentrations of Ag in soils sampled at the start of the earthworm uptake experiment with ionic Ag and Ag nanoparticles (AgNPs)[a]

Ag compound	Ag nominal (mg kg^{-1})	Total actual [Ag] (mg kg^{-1})	% recovery	Ag porewater (mg L^{-1})
$AgNO_3$	20 ($n = 3$)	23.5 ± 2.48	117	0.03 ± 0.01
	100 ($n = 3$)	101 ± 4.42	100	0.26 ± 0.02
AgNPs	100 ($n = 6$)	84.9 ± 33.8	85.0	0.024 ± 0.001
	500 ($n = 6$)	431 ± 115	86.3	0.044 ± 0.001

[a]Data are mean values ± standard deviations (SDs).

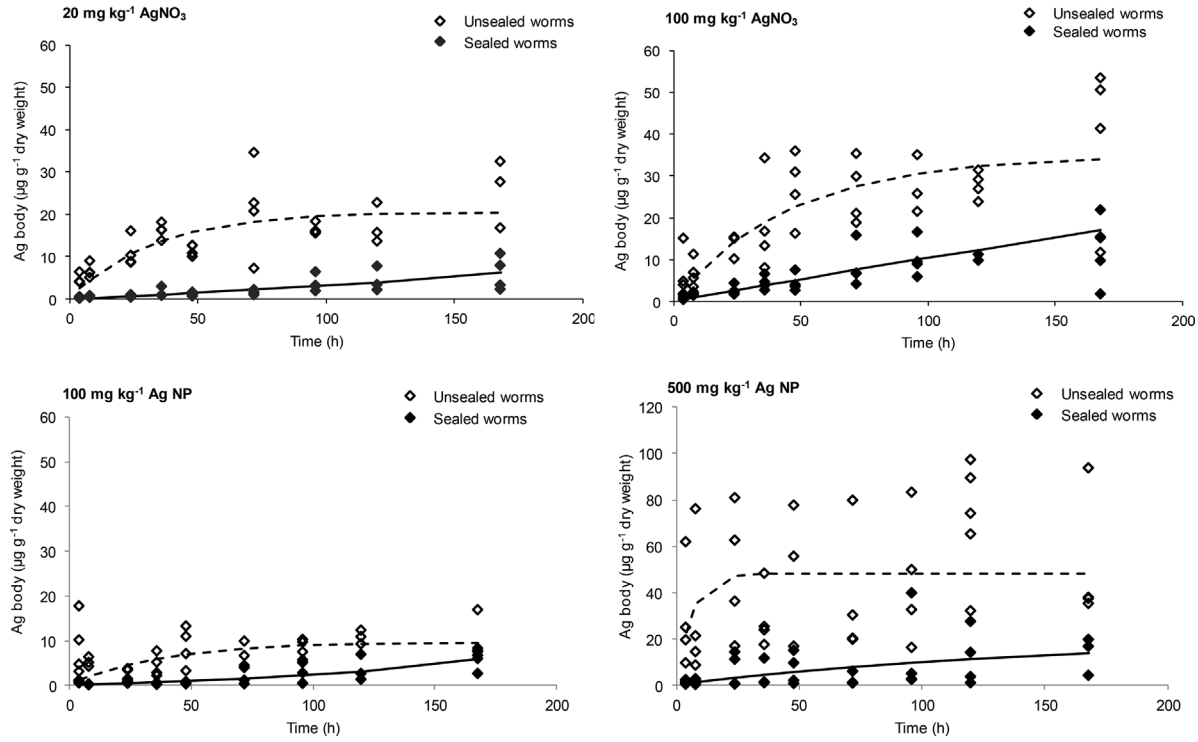

Figure 1. Total Ag concentrations in tissues (µg g^{-1} dry wt) of *Lumbricus rubellus* exposed to Ag^+ ions ($AgNO_3$, exposure concentration: 20 mg kg^{-1} and 100 mg kg^{-1} dry wt) and Ag nanoparticles (AgNPs; exposure concentration: 100 mg kg^{-1} and 500 mg kg^{-1} dry wt) in LUFA 2.2 loam sand soil (points indicate measured concentrations for individual earthworms; dashed and solid lines indicate 1-compartment model fit to Ag uptake by unsealed and sealed worms, respectively). Note differences in scales of vertical axes.

observed (after removal of interference from the strong Ar Kβ signal predominantly in: (i) the chloragogenous tissue within the typhlosole and (ii) around the basal intestinal surface; (iii) nephridial tubules and (iv) near the base of setae of the AgNP-exposed specimen (Figure 2A). Because of the spectral manipulation required to create the fluorescent maps, which limited identification by mapping, the presence of Ag at these probable sequestration sites was confirmed by the acquisition of short XANES scans across the Ag L(II)-edge, and observing the sharp increase in intensity at the characteristic energy of the Ag L(II)-edge at these locations, as shown in the XANES scans (Figure 2C, spectra i–iv). Fluorescence mapping and XANES scanning under identical microfocus conditions and in equivalent tissue structures (spectra v–viii, Figure 2D) at locations v–viii in

Table 2. Uptake and elimination rate constants estimated from 1-compartment model fits of a time series of total body Ag concentrations measured in the earthworm *Lumbricus rubellus* exposed to Ag^+ ions and Ag nanoparticles (AgNPs) in LUFA 2.2 loam sand soil[a]

Ag nominal (µg g^{-1})	Treatment	$k_{1\text{-T}}$ (g soil earthworm^{-1} h^{-1})	$k_{2\text{-T}}$ (h^{-1})	$k_{1\text{-pw}}$ (g soil g earthworm^{-1} hour^{-1})	r^2
20 mg kg^{-1} $AgNO_3$	Unsealed	0.03 A (0.02–0.04)	0.031 (0.01–0.05)	21.0 A (12.3–29.8)	0.705
	Sealed	0.0012 B (0.0005–0.002)	0 (-)[b]	0.83 B (0.32–1.33)	0.631
100 mg kg^{-1} $AgNO_3$	Unsealed	0.008 C,I (0.004–0.011)	0.022 (0.009–0.035)	2.94 C,I (1.73–4.15)	0.706
	Sealed	0.001 B,I (0.001–0.001)	0.001 (0–0.006)	0.51 B (0.32–0.69)	0.815
100 mg kg^{-1} AgNPs	Unsealed	0.002 A,II ($4x10^{-4}$–0.004)	0.026 (0–0.055)	10.5 A,II (2.09–18.8)	0.550
	Sealed B,II	$1.2x10^{-4}$ B,II ($15x10^{-5}$–$2.3^{*}10^{-4}$)	0 (-)[b]	0.53 B (0.06–0.98)	0.637
500 mg kg^{-1} AgNPs	Unsealed	0.015 A (0.002–0.033)	0.160 (0–0.350)	177 C (21–376)	0.290
	Sealed	$3x10^{-4}$ B ($4.3x10^{-5}$–0.001)	0.0063 (0–0.029)	2.99 B (0.49–6.49)	0.637

[a]Constants relate to total ($k_{1\text{-T}}$ and $k_{2\text{-T}}$) and soil porewater ($k_{1\text{-pw}}$) silver concentrations. The 95% confidence intervals are shown in parentheses. The coefficient of determination (r^2) describes variance in earthworm body concentrations of Ag explained by the fitted model. A, B, and C indicate significant differences between k_1 values for each compound for the different treatments (sealed and unsealed) and different exposure concentrations according to a generalized likelihood-ratio test ($X^2(1) > 3.84$; $p < 0.05$). I and II indicate significant differences between k_1 values for each exposure concentration according to a generalized likelihood-ratio test ($X^2(1) > 3.84$; $p < 0.05$). Data did not allow the calculation of reliable 95% confidence intervals.

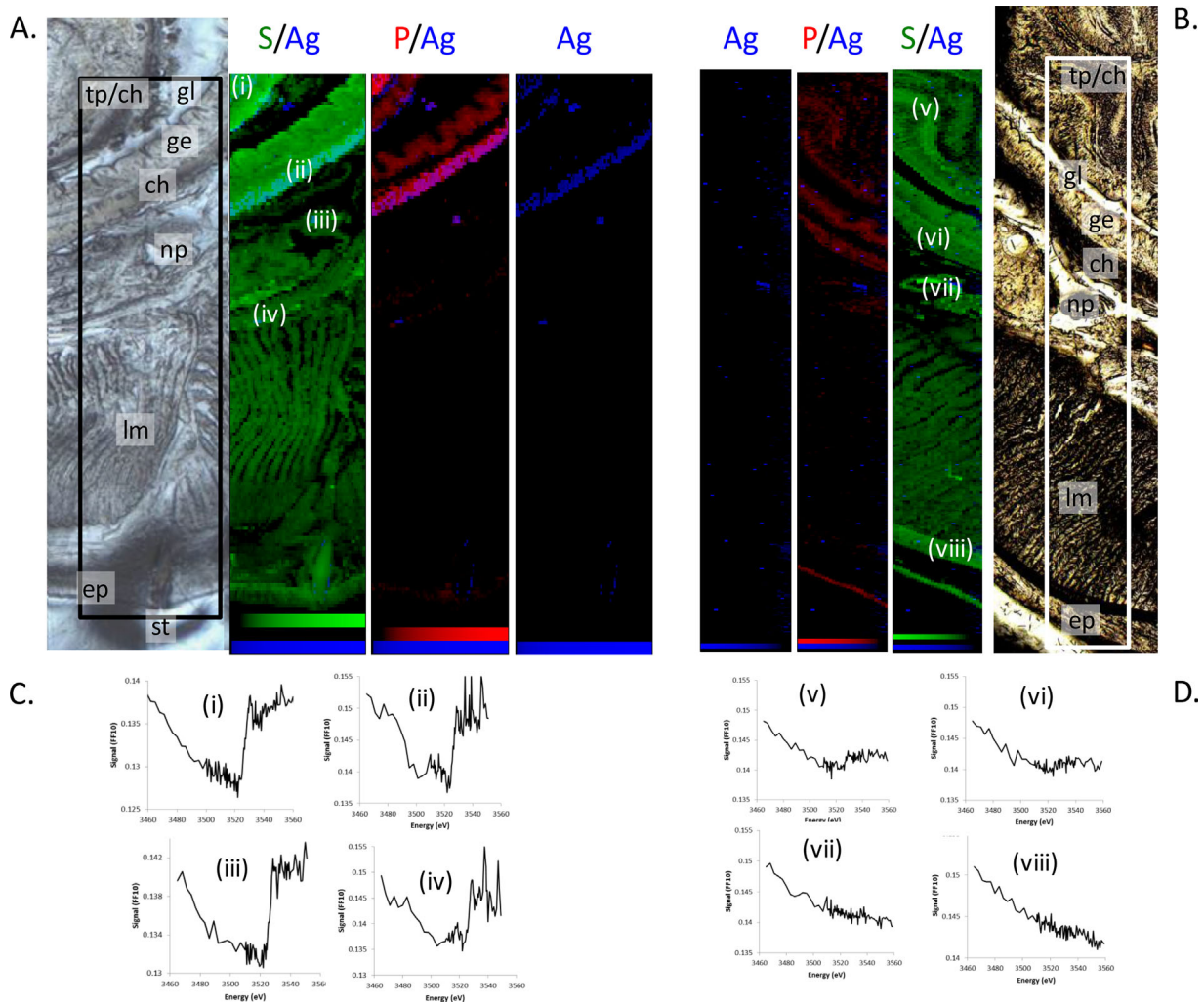

Figure 2. μX-ray fluorescence maps and Ag L(II)-edge spectra derived from histological sections of earthworms exposed to silver nanoparticles (AgNPs) and Ag ions. Sections were generated from alcohol-fixed, methacrylate-embedded, transverse sections of mouth-unsealed earthworms (*Lumbricus rubellus*) exposed to 500 mg Ag kg^{-1} applied in the form of AgNPs (**A** and **C**) and 100 mg Ag kg^{-1} in the form of Ag^{+} ions (**B** and **D**). For each of the treatments we have provided unstained light microscopic images of the transverse sections labeling all the major anatomical features of the earthworm (key given below). We have also included binary overlays of sulfur (green) and silver (blue), and phosphorus (red) and silver (blue), as well as silver alone (blue). The relative fluorescence of each element is represented on a log scale between 0 RFU and 140 000 RFU with a scale bar for the individual elements provided at the base of each image. The locations used for Ag L(II)-edge spectra are labeled (i)–(iv), shown in **C** for the AgNP sample, and (v)–(viii), shown in **D** for the Ag-Ion sample. Anatomical labels used include: ep = epithelium; cm = circular muscle; lm = longitudinal muscle; ch = chloragogenous tissue; ge = gut (intestinal) epithelium; gl = gut lumen; lm = longitudinal muscle; np = nephridial tubule profiles (in the coelomic cavity); ty = typhlosole fold (with enclosed chloragog).

the ion-exposed specimen (center) was unable to detect Ag in the earthworm.

DISCUSSION

The successful application of models such as the free ion activity model and BLM to explain the effects of variations in media properties on metal toxicity [15–17] has pointed to the validity of the assumptions of these models that relate to the concentration of the ionic form in contact with external surfaces (epidermis, gill). Attempts to apply models such as the BLM that assume dermal interactions with the dissolved metal to explain observed metal uptake and toxicity in soil-dwelling organisms have generally been informative [15,16]. Such assessments could be taken as an indication of exposure to the free dissolved ion occurring primarily through contact of external surfaces such as the body wall with the external media: notably the soil solution, because this is an assumption inherent in these models. So far, application of the free ion activity model and BLM to explain the effects of metals on soil organisms has not extended to studies with Ag. Further examples of the application of these 2 models to explain effects of metal and metal oxide-based NPs are currently not available. The present studies on the relevance of different exposure routes for Ag ions and AgNP uptake by earthworms are informative for the validity of such future applications.

For geophagous groups such as earthworms, the gut-lining, like the skin, will be in near continuous contact with the soil medium. Hence for these species, exposure to metal ions and other metal forms, including intact NPs, from the diet is a clear possibility. Such intake via the gut provides the potential for exposure that may be additional to that resulting from dermal contact alone [9]. As many soil organisms live in and also consume the soil (and associated contaminants), disentangling the contribution of different exposure routes to uptake can be challenging. For example, even if gut exposure is actually an important site of uptake, deviations of accumulation rates from those derived from only epidermal exposure will only occur if

the gut physiology has a substantive influence on the rates of metal ion association with uptake sites or, alternatively, if the frequency of uptake sites in gut tissues exceeds that of the epidermis. If such differences are not the case, then metal transport over the body wall and gut epithelium will be effectively equivalent.

To tease apart the contributions of different routes for chemical uptake by earthworms, a number of different approaches such as ligature [9] and oral gluing [10] to inhibit feeding have been applied. In the latter seminal study, gluing was suggested as a suitable approach for oral sealing, as it allowed normal burrowing and behavior in the absence of feeding. This suggestion is confirmed by observations made in the present study. Thus the sealed *L. rubellus* showed no physical signs of skin irritation from the procedure, and features such as mucus production did not interfere with the setting of the glue. Furthermore, during the experiments, earthworm burrowing behavior, physical appearance, and survival were all normal. Thus, even though the sealing of the anterior end could have been potentially stressful, these effects did not appear to influence key physiological and behavioral parameters that could have affected metal uptake.

The present study is to our knowledge the first to separate exposure routes for both the Ag ion and AgNPs (or indeed any nanoparticle) in a soil exposure experiment. Thus we provide a unique view of the role of different exposure routes for 2 different untested cases. The results for both the Ag ion and AgNPs point to the relative importance of the intestinal route for Ag uptake, with oral sealing reducing Ag assimilation by between 40% and 75% in all 4 cases (2 Ag^+ ion concentrations, 2 AgNP concentrations; Figure 1). The relative contributions of the 2 exposure routes, most notably the dominance of oral exposure, were similar whether exposure was to Ag^+ ions or AgNPs. As the concentrations used in the present study were above current anticipated environmental concentrations [32], they need to be validated at lower concentrations. However, because no physiological effects were seen, it may not be anticipated that behavior or physiological difference would change uptake patterns at lower exposure concentrations.

The physiological basis for the dominance of Ag assimilation principally through the intestine, rather than the dermal route that appears dominant for other metals [10], remains open to speculation. This is compounded by the fact that in NP exposure, it is not certain whether accumulation is of intact NPs, released metal ions, or both. One contributing factor could be the strong affinity of Ag^+ for soil organic matter [33]. This results in relatively low concentrations of free Ag^+ ions in soil porewater. When this organic matter is consumed, the presence of surfactant molecules and other conditions within the gut lumen may possibly allow the greater release of Ag into solution that may then be assimilated. Because the stability of AgNPs in solution can be influenced by the presence of molecules such as surfactant molecules [34,35], similar processes may affect NP assimilation. Alternative suggestions to explain preferential Ag^+ ion and AgNP uptake in the gut could include a greater representation of key receptors for Ag such as the Na^+/K^+ ATPase in the gut lining compared with the body wall, or a specific speciation chemistry of Ag under the specific redox and solute conditions associated with the earthworm gut and its microbial community that particularly facilitate uptake.

To confirm whether the measured total Ag concentration in earthworms is actually internalized by cells and tissues, and not merely associated by adsorption onto dermal and gut epithelial surfaces, in situ Ag distribution mapping using synchrotron-beam microfocus imaging and analysis was carried out on unsealed earthworms exposed to the highest concentrations of Ag^+ ions and AgNPs. The fate of assimilated Ag within earthworms showed a qualitative difference depending on the chemical form of Ag to which they were exposed. The Ag was detectable in setae (hair) follicles, chloragogenous tissue, and nephridia after 168 h of exposure to AgNPs, but could not be detected in any tissue of Ag^+ ion-exposed earthworms. The difference is not easy to explain, especially because our bulk chemistry observations indicate that Ag is more readily accumulated when the exposure is to Ag^+ ions compared with AgNPs.

Our microfocus observations on AgNP-exposed earthworms suggest that the mechanism, if not the anatomical route, of AgNP uptake could differ from that of Ag^+ ions. The Ag was not adsorbed onto epidermal and epithelial surfaces. Indeed, the highly focal distribution of Ag in NP-exposed earthworm tissues implies that the metal was internalized mainly, if not exclusively, to local hotspots, potentially as intact NPs via endocytosis pathways in intestinal epithelia. This finding could support the identification of the gut as the major route of Ag uptake by earthworms as derived from the toxicokinetics studies of oral sealed and unsealed earthworms. This aspect, however, requires further confirmation from additional imaging and mechanistic studies. Whether the detection of Ag near the base of the setae is also indicative of a hitherto unsuspected route of transepidermal uptake, or a means of NP excretion analogous to the recently identified hair follicle route in mammals [36], also warrants further study.

The identification of the gut as the dominant route of uptake of Ag as ion and NPs has a number of specific implications for the way these chemicals can be handled within risk assessment. A current focus in metal and NP ecotoxicological research is to understand how environmental conditions such as pH and organic matter, and also for NPs relevant processes such as aggregation and dissolution, are related to toxicity. Models of ionic metal toxicity, such as the BLM, have been used to account for soil and water chemistry influences on toxicity, and it has been proposed that such models could be useful for predicting the toxicity of metals and metal oxide NPs [37]. The BLM relies on a mechanistic assumption that the toxic effect is driven by the concentration of the free ion, as derived from measurement, which is able to bind to a relevant receptor (the biotic ligand) after the competing effects of other cations on receptor occupancy have been taken into account. For NPs subject to dissolution, the relevance of the BLM for dissolved ions has been suggested. However, application to intact NPs themselves has yet to be demonstrated [38]. Principles for the application of the BLM implicitly assume exposure via the soil solution principally via external organs such as the body wall and respiratory surfaces. The results presented in the present study, however, suggest that dermal exposure may not be the only, or even the most important, route of exposure for both Ag^+ ions and AgNPs for earthworms. Inclusion of exposure and subsequent tissue distribution through the gut is also necessary to fully account for exposure effects on toxicity. Given that the gut surface, like the skin, is in near continuous contact with the soil, this consideration may not actually require extensive modification of the BLM if the physicochemical conditions for uptake across both are similar. However, if gut chemical conditions or physiology are different from those of the bulk soil and skin, then this would require specific consideration in exposure modeling. Regardless of the actual mechanism(s) involved, our results show that dietary uptake of NPs is a route of exposure that should be considered in risk assessments, bioavailability, and modeling of metal-based NP.

Acknowledgment—The authors acknowledge R.A. Verweij at the VU University in Amsterdam for help and guidance with metal analysis. M. Diez-Ortiz was supported by a Marie Curie Intra-European Fellowship within the 7th European Community Framework Programme (call reference FP7-PEOPLE-2010-IEF, 273207 Nano-Ecotoxicity). A.J. Morgan and P. Kille are grateful to Diamond Light Source for 2 Beamtime Awards (SP7837-1 and SP7837-2), as well as valuable technical advice from T. Geraki. D.J. Spurgeon, E. Lahive, A. John Morgan, K. Jurkschat, K. Powell, C.A.M. Van Gestel, and C. Svendsen received financial support from NanoFATE, Project CP-FP 247739 (2010-2014) under the 7th Framework Programme of the European Commission (FP7-NMP-ENV-2009, Theme 4; www.nanofate.eu).

Data availability—Data, associated metadata, and calculation tools may be requested from the authors (mdiez@leitat.org).

REFERENCES

1. Kiser MA, Westerhoff P, Benn T, Wang Y, Perez-Rivera J, Hristovski K. 2009. Titanium nanomaterial removal and release from wastewater treatment plants. *Environ Sci Technol* 43:6757–6763.
2. Johnson AC, Bowes MJ, Crossley A, Jarvie HP, Jurkschat K, Juergens MD, Lawlor AJ, Park B, Rowland P, Spurgeon D, Svendsen C, Thompson IP, Barnes RJ, Williams RJ, Xu N. 2011. An assessment of the fate, behaviour and environmental risk associated with sunscreen TiO2 nanoparticles in UK field scenarios. *Sci Total Environ* 409:2503–2510.
3. Colman BP, Arnaout CL, Anciaux S, Gunsch CK, Hochella MF, Jr., Kim B, Lowry GV, McGill BM, Reinsch BC, Richardson CJ, Unrine JM, Wright JP, Yin L, Bernhardt ES. 2013. Low concentrations of silver nanoparticles in biosolids cause adverse ecosystem responses under realistic field scenario. *PLoS One* 8:e57189.
4. Coutris C, Hertel-Aas T, Lapied E, Joner EJ, Oughton DH. 2012. Bioavailability of cobalt and silver nanoparticles to the earthworm *Eisenia fetida*. *Nanotoxicology* 6:186–195.
5. Kool PL, Ortiz MD, van Gestel CAM. 2011. Chronic toxicity of ZnO nanoparticles, non-nano ZnO and ZnCl2 to *Folsomia candida* (Collembola) in relation to bioavailability in soil. *Environ Pollut* 159:2713–2719.
6. Unrine JM, Hunyadi SE, Tsyusko OV, Rao W, Shoults-Wilson WA, Bertsch PM. 2010. Evidence for bioavailability of Au nanoparticles from soil and biodistribution within earthworms (*Eisenia fetida*). *Environ Sci Technol* 44:8308–8313.
7. Heggelund L, Diez-Ortiz M, Spurgeon DJ, Svendsen C. 2013. Soil pH effects on the comparative toxicity of dissolved zinc, non-nano and nano ZnO to the earthworm *Eisenia fetida*. *Nanotoxicology* 5:559–572.
8. Jager T, Albert C, Preuss TG, Ashauer R. 2011. General unified threshold model of survival—A toxicokinetic-toxicodynamic framework for ecotoxicology. *Environ Sci Technol* 45:2529–2540.
9. Jager T, Fleuren R, Hogendoorn EA, De Korte G. 2003. Elucidating the routes of exposure for organic chemicals in the earthworm, *Eisenia andrei* (Oligochaeta). *Environ Sci Technol* 37:3399–3404.
10. Vijver MG, Vink JPM, Miermans CJH, Van Gestel CAM. 2003. Oral sealing using glue: A new method to distinguish between intestinal and dermal uptake of metals in earthworms. *Soil Biol Biochem* 35:125–132.
11. Morel FMM, Hering JG. 1983. *Principles of Aquatic Chemistry*. John Wiley & Sons, New York, NY, USA.
12. Di Toro DM, Allen HE, Bergman HL, Meyer JS, Paquin PR, Santore RC. 2001. Biotic ligand model of the acute toxicity of metals. 1. Technical basis. *Environ Toxicol Chem* 20:2383–2396.
13. Lofts S, Spurgeon D, Svendsen C. 2005. Fractions affected and probabilistic risk assessment of Cu, Zn, Cd, and Pb in soils using the free ion approach. *Environ Sci Technol* 39:8533–8540.
14. Lofts S, Criel P, Janssen CR, Lock K, McGrath SP, Oorts K, Rooney CP, Smolders E, Spurgeon DJ, Svendsen C, Van Eeckhout H, Zhao FZ. 2013. Modelling the effects of copper on soil organisms and processes using the free ion approach: Towards a multi-species toxicity model. *Environ Pollut* 178:244–253.
15. Thakali S, Allen HE, Di Toro DM, Ponizovsky AA, Rooney CP, Zhao FJ, McGrath SP, Criel P, VanEeckhout H, Janssen CR, Oorts K, Smolders E. 2006. Terrestrial biotic ligand model. 2. Application to Ni and Cu toxicities to plants, invertebrates, and microbes in soil. *Environ Sci Technol* 40:7094–7100.
16. Le TTY, Peijnenburg W, Hendriks AJ, Vijver MG. 2012. Predicting effects of cations on copper toxicity to lettuce (*Lactuca sativa*) by the biotic ligand model. *Environ Toxicol Chem* 31:355–359.
17. Lofts S, Spurgeon DJ, Svendsen C, Tipping E. 2004. Deriving soil critical limits for Cu, Zn, Cd and Pb: A method based on free ion concentrations. *Environ Sci Technol* 38:3623–3621.
18. Cain D, Croteau M-N, Luoma S. 2011. Bioaccumulation dynamics and exposure routes of Cd and Cu among species of aquatic mayflies. *Environ Toxicol Chem* 30:2532–2541.
19. Simkiss K, Watkins B. 1990. The influence of gut microorganisms on zinc uptake in *Helix aspersa*. *Environ Pollut* 66:263–271.
20. Hopkin SP. 1990. Species-specific differences in the net assimilation of Zn, Cd, Pb, Cu and Fe by the terrestrial isopods *Oniscus asellus* and *Porcellio scaber*. *J Appl Ecol* 27:460–474.
21. Poteat MD, Buchwalter DB. 2014. Four reasons why traditional metal toxicity testing with aquatic insects is irrelevant. *Environ Sci Technol* 48:887–888.
22. Hooper HL, Jurkschat K, Bailey J, Morgan AJ, Lawlor AJ, Spurgeon D, Svendsen C. 2011. Comparative chronic toxicity of nanoparticulate and ionic zinc to the earthworm *Eisenia veneta* in a soil matrix. *Environ Int* 37:1111–1117.
23. Novak S, Drobne D, Goobic M, Zupanc J, Romih T, Gianoncelli A, Kiskinova M, Kaulich B, Pelicon P, Vavpetic P, Jeromel L, Ogrinc N, Makovec D. 2013. Cellular internalization of dissolved cobalt ions from ingested CoFe2O4 nanoparticles: *In vivo* experimental evidence. *Environ Sci Technol* 47:5400–5408.
24. Løkke H, Van Gestel CAM. 1998. *Handbook of Soil Invertebrate Toxicity Tests*. John Wiley & Sons, Hoboken, NJ, USA.
25. Shoults-Wilson WA, Reinsch BC, Tsyusko OV, Bertsch PM, Lowry GV, Unrine JM. 2011. Effect of silver nanoparticle surface coating on bioaccumulation and reproductive toxicity in earthworms (*Eisenia fetida*). *Nanotoxicology* 5:432–444.
26. Waalewijn-Kool PL, Ortiz MD, Van Straalen NM, Van Gestel CAM. 2013. Sorption, dissolution and pH determine the long-term equilibration and toxicity of coated and uncoated ZnO nanoparticles in soil. *Environ Pollut* 178:59–64.
27. Organisation for Economic Co-operation and Development. 2004. Guideline for the testing of chemicals No. 222. Earthworm reproduction test (*Eisenia fetida/Eisenia andrei*). Paris, France.
28. Mosselmans JFW, Quinn PD, Dent AJ, Cavill SA, Moreno SD, Peach A, Leicester PJ, Keylock SJ, Gregory SR, Atkinson KD, Rosell JR. 2009. I18—The microfocus spectroscopy beamline at the Diamond Light Source. *J Synchrotron Radiat* 16:818–824.
29. Sole VA, Papillon E, Cotte M, Walter P, Susini J. 2007. A multiplatform code for the analysis of energy-dispersive X-ray fluorescence spectra. *Spectrochim Acta B Atomic Spectrosc* 62:63–68.
30. Sokal RR, Rohlf FJ. 1994. *Biometry: Principles and Practice of Statistics in Biological Research*, 3rd ed. Freeman, London, UK.
31. Diez-Ortiz M, Lahive E, George S, Ter Schure A, Van Gestel CAM, Jurkschat K, Svendsen C, Spurgeon DJ. 2015. Short-term soil bioassays may not reveal the full toxicity potential for nanomaterials; bioavailability and toxicity of silver ions ($AgNO_3$) and silver nanoparticles to earthworm *Eisenia fetida* in long-term aged soils. *Environ Pollut* 203:191–198.
32. Gottschalk F, Sonderer T, Scholz RW, Nowack B. 2009. Modeled environmental concentrations of engineered nanomaterials (TiO_2, ZnO, Ag, CNT, Fullerenes) for different regions. *Environ Sci Technol* 43:9216–9222.
33. Coutris C, Joner EJ, Oughton DH. 2012. Aging and soil organic matter content affect the fate of silver nanoparticles in soil. *Sci Total Environ* 420:327–333.
34. Chappell MA, Miller LF, George AJ, Pettway BA, Price CL, Porter BE, Bednar AJ, Seiter JM, Kennedy AJ, Steevens JA. 2011. Simultaneous dispersion-dissolution behavior of concentrated silver nanoparticle suspensions in the presence of model organic solutes. *Chemosphere* 84:1108–1116.
35. Ruge CA, Schaefer UF, Herrmann J, Kirch J, Canadas O, Echaide M, Perez-Gil J, Casals C, Muller R, Lehr CM. 2012. The interplay of lung surfactant proteins and lipids assimilates the macrophage clearance of nanoparticles. *Plos One* 7:e40775.
36. Kempson IM, Chien C-C, Chung C-Y, Hwu Y, Paterson D, de Jonge MD, Howard DL. 2012. Fate of intravenously administered gold nanoparticles in hair follicles: Follicular delivery, pharmacokinetic interpretation, and excretion. *Adv Healthcare Mater* 1:736–741.
37. Fabrega J, Luoma SN, Tyler CR, Galloway TS, Lead JR. 2011. Silver nanoparticles: Behaviour and effects in the aquatic environment. *Environ Int* 37:517–531.
38. Choi O, Cleuenger TE, Deng B, Surampalli RY, Ross L, Jr., Hu Z. 2009. Role of sulfide and ligand strength in controlling nanosilver toxicity. *Water Res* 43:1879–1886.